A New Finite Difference Scheme for Three Dimensional Advection

Gary L. Russell

NASA Goddard Institute for Space Studies
Goddard Space Flight Center
New York, New York

and

Jean A. Lerner

Sigma Data Services Corporation
2880 Broadway
New York, New York

ABSTRACT

A new scheme of advecting tracers by general circulation model winds is presented. Within each model grid box, the scheme calculates the mean concentration, and, in addition, the linear slope of concentration for the east-west, north-south, and vertical directions. This slopes scheme yields much smoother and thus more realistic tracer distributions than either second or fourth order schemes, and it is relatively non-diffusive. The upstream scheme and the three already mentioned schemes are compared in one and two dimensions with constant winds. In three dimensions, five month simulations of carbon monoxide with model predicted winds are shown.

INTRODUCTION

The general circulation climate model under development at the Goddard Institute for Space Studies has the ability to carry four 'tracers' on-line. The tracers are quantities which are advected by the winds, mixed by convection, and changed by calculated sources and sinks, but do not affect the model's simulated climate. We can also save, on a computer tape, the monthly mixing by convection, and, every six hours, the time averaged winds over that interval. In that way we can make several tests of the tracer part of the model without recomputing the whole model. Normally we run the tracers in this off-line mode.

The purpose of this paper is to examine several advection schemes for tracers to be used in conjunction with the winds generated by our three dimensional climate model.

THE WELL KNOWN SCHEMES

At first we considered three well known advective schemes: the upstream scheme, the second order scheme, and the fourth order scheme. The first two schemes are described in Figures 1 and 2. The fourth order scheme does not lend itself to a similar schematic figure. But using the same definitions as those used in Figure 1, the fourth order scheme (in one dimension) calculates the mean concentration of grid box i at the end of a time step as

$$[R_i + \alpha(-R_{i-2}+7R_{i-1}+7R_i-R_{i+1})/12 - \beta(-R_{i-1}+7R_i+7R_{i+1}-R_{i+2})/12]/(1+\alpha-\beta).$$

We should note that in all our tests, the mass flux of air crossing an interface is predetermined. The current version of our general circulation model, which generates the mass fluxes for our three dimensional tests, uses second order differencing.

The deficiencies of each of these schemes are well known. The upstream scheme is highly diffusive. While the second and fourth order schemes are inherently non-diffusive, negative concentrations occur with both, and adjustments to prevent these negative concentrations cause diffusion. The second order scheme does not advect the peak concentration as well as do the other schemes. In three dimensions, both the second and fourth order schemes create a noisy pattern with unrealistic gradients.

THE SLOPES SCHEME

The slopes scheme is basically an upstream scheme but uses, for each grid box, the mean concentration and the linear slope of concentration for the east-west, north-south, and vertical directions. In each dimension, the distribution within a grid box plus the distribution of the incoming air minus that of the outgoing air during a time step are fitted by the root mean square line to determine the linear distribution of concentration for the next step. Figure 3 describes the slopes scheme in one dimension, but that prescription is applied to all three dimensions.

The non-diffusive character of the scheme and its ability to advect tracer distributions accurately will be obvious from our several tests.

PREVENTING NEGATIVE CONCENTRATIONS

Starting from a non-uniform tracer distribution, it is possible that numerical schemes will cause negative concentrations. There are several different reasons for such occurrences.

Negative concentrations can result if the mass of air leaving several faces of a grid box during a time step exceeds the mass of air in the box. (Although there will be air entering the grid box through other faces, the tracer concentration of the incoming air may be insignificant). The small time step required when dynamically integrating a GCM prevents this problem from occurring when a tracer is run on-line. However, when a tracer is run off-line, one typically uses a longer time step. In the upstream and slopes schemes we limit the mass of air leaving any face of a grid box during a time step to 1/2 the mass of air in the box. That limit effectively eliminates negative concentrations.

The second and fourth order schemes require a more stringent test. Even if the mass of air leaving one face of a grid box is small, it could take with it a large mass of tracer, leaving a deficit in the box. One way to prevent this is the 'filling' method of 'downstream borrowing' (Mahlman [1]). We, however, use a simpler calculation wherein the mass of tracer leaving any face of a grid box during a time step is limited to 1/2 of the current mass of tracer in the box.

Since we advect separately in the three dimensions, our limit prevents negative concentrations.

We should note that the 'downstream borrowing' method as used by Mahlman [1] would be invoked less often than our method, and consequently would have less numerical distortion. However, based on tests we have run with Mahlman's formulation in our one dimensional model, we believe the differences should be insignificant.

The final source of negative concentrations applies to the slopes scheme only. If the magnitude of the slope in any direction is sufficiently large, it is possible to have negative concentrations near the faces of a grid box. This can cause mean concentrations in neighboring boxes to become negative. To prevent this, we limit the magnitude of each slope so that the concentration at any face is greater than zero and less than two times the mean concentration.

Table I shows the frequencies at which these limits are invoked for the fifth month of our three dimensional tests. They are global numbers in percent, and are of course time step dependent. Except for the slopes limit, the east-west frequencies generally increase with latitude.

TIME STEPS

The second and fourth order schemes use leap frog time-stepping. The leap frog is started by a single forward explicit step. In the two and three dimensional tests, we stop the leap frog at regular intervals and then restart it with a single forward step. For the upstream and slopes scheme, leap frog is unnecessary. Hence, they use forward explicit steps only.

TESTS IN ONE DIMENSION

Our one dimensional model uses 36 grid boxes around a circle with all boxes having equal mass and equal length Δx. The wind speed u is constant in space and time, and the time step Δt is constant in time. The only essential parameter is $\gamma = u \cdot \Delta t/\Delta x$ which is dimensionless. For all the tests shown, $\gamma = 1/8$. For smaller γ, all the schemes are essentially unchanged. For larger γ, the upstream and slopes schemes have slight improvements whereas the second and fourth order schemes are degraded because of our limits imposed to avoid negative concentrations. The initial tracer distribution is a wedge (see Figure 4) which has been used by several authors, e.g. Mahlman and Sinclair [2]. For the slopes scheme, the initial slopes must also be specified; we set them to zero.

The results of advecting the wedge around the circle five times with each of the four schemes are shown in Figure 5. A perfect scheme would keep the wedge intact. In the computations for Figures 5 and 6 we use our stated limits to prevent negative concentrations. It is clear that the upstream scheme is highly diffusive. The second order scheme misplaces and rounds off the peak. Both the fourth order and slopes schemes advect the wedge rather accurately.

Figure 6 shows the tracer distributions produced by the four schemes after advecting the initial distribution fifty times around the circle. With the upstream scheme,

the tracer distribution has become uniform. The second order scheme is also diffusive and its peak is, of course, misplaced. The fourth order scheme has some diffusion, a secondary maximum, and its peak is slightly off center. The slopes scheme is still accurately advecting the wedge but some diffusion has crept in.

We have also tested the schemes without imposing our limits, thus allowing negative concentrations. Figure 7 shows the results after fifty revolutions. For the upstream scheme, Figures 6 and 7 are identical. The second order scheme yields a meaningless distribution. The magnitude of the peak is good with the fourth order scheme, but its location is slightly misplaced and the scheme has secondary maxima and minima. The slopes scheme is very smooth and its peak is positioned correctly, but its magnitude is less than that of the fourth order scheme.

With each of the schemes, the mass of tracer is conserved with time, i.e., $\sum_{i=1}^{36} R_i = 50$. We also calculate the R^2 norm, $\sum_{i=1}^{36} R_i^2$, as a function of time. It measures the amount of diffusion for a given scheme. For a perfectly non-diffusive scheme the R^2 norm would remain constant. Figure 8 shows the R^2 norm for the four schemes using our stated limits to prevent negative concentrations. The slopes scheme has a quick decrease because the initial slopes were set to zero. With no limits, the R^2 norm for the upstream scheme would be unchanged, for the second and fourth order schemes

the R^2 norm would be constant at 340, and for the slopes scheme it would be somewhat greater than it is in Figure 8, reaching a value of 254 after 30 revolutions.

TESTS IN TWO DIMENSIONS

The two dimensional model uses the same idea as that of our one dimensional model. A regular latitude-longitude map divides up the surface of a sphere into 36 grid boxes from west to east and 24 grid boxes from north to south. The 36 grid boxes adjoining a pole are merged into a single grid box. The constant winds are specifed so as to rotate air around a fixed axis with a constant angular velocity. The winds are defined at the corners of the grid boxes.

An ideal scheme would keep the initial tracer distribution intact and unchanged after many revolutions. In reality this cannot happen because of errors in the scheme and because of the finite mesh at which the wind points are defined; certain grid boxes are constantly accumulating air and other are losing air. To correct this problem, the concentration at the beginning of a time step is set equal to the concentration at the end of the previous step, but air is redistributed so that it is proportional to the area of each grid box. This readjustment should not affect the relative performance of the different schemes.

For the upstream and slopes schemes, the time step is 1/432 of a full revolution. Multiplying by the number of grid boxes in the east-west direction gives 1/12, which compares with $Y = 1/8$ in the one dimensional tests. The second and fourth order schemes use a time step of 1/1728 of a full revolution; or 1/48 per grid box. The smaller time step

reduces the frequency of invoking our limits preventing negative concentrations. All schemes for the two dimensional tests use the limits described above.

The initial tracer distribution for our two dimensional tests is shown in Figure 9. The symbols used to specify the concentration within the 24 by 36 matrix of grid boxes use a logarithmic base 2 scale:

0 = 0 → 1	7 = 64 → 128	E = 81922 → 16384
1 = 1 → 2	8 = 128 → 256	F = 16384 → 32768
2 = 2 → 4	9 = 256 → 512	G = 32768 → 65536
3 = 4 → 8	A = 512 → 1024	H = 65536 → 131072
4 = 8 → 16	B = 1024 → 2048	I = 131072 → 262144
5 = 16 → 32	C = 2048 → 4096	
6 = 32 → 64	D = 4069 → 8192	

Remember the top row matrix entries and bottom row entries correspond to single polar grid boxes. For Figure 9, a value of tracer concentration of zero for a grid box is blanked out. For Figures 10 and 11, values from 32 to 1024 are blanked out in order to better discern the problems with the schemes. The average area weighted tracer concentration over the globe is 1000.

For the slopes scheme, the two polar grid boxes do not use or calculate a horizontal slope; the horizontal concentration is always uniform. At the initial time, all slopes are set to zero.

Figure 10 shows the tracer distribution after advecting the initial state twice around the globe. The upstream scheme is very diffusive, but it does accurately predict the position of maximum concentration. The second order scheme does not position the peak as well as the other schemes. The fourth order scheme shows an unrealistic wave pattern, but the peak concentration is larger and thus more accurate than it is for the other schemes. The slopes scheme yields a tracer distribution which is very smooth and quite realistic in other respects.

Figure 11 shows the tracer distributions after ten revolutions. The upstream scheme has dispersed the tracer almost to the point of homogeniety. The peak concentration for the second order scheme lags behind its correct location and the distribution is smeared over several grid boxes. The fourth order scheme has a large peak at an accurate position; its main deficiency is the persistent wave pattern. The peak concentration for the slopes scheme is less than that of the fourth order scheme but in other respects the slopes scheme does a good job.

THREE DIMENSIONAL TESTS WITH CARBON MONOXIDE

We saved on a computer tape the winds generated by our three dimensional climate model. The model is a sigma coordinate GCM with seven vertical layers and 8° by 10° horizontal resolution. The winds were averaged over 6 hour intervals. For these tests there was no mixing by convection.

The tracer model was run off-line with carbon monoxide as the trace constituent. The model included a realistic anthropogenic source over industrial areas and an equatorial plant source, both of which were released into the bottom layer. There was a photo-chemical destruction rate proportional to the current concentration of CO and an independent photo-chemical production rate, both of which affect all layers.

The initial conditions for these tests were generated by running the slopes scheme for 2 years starting from a uniform CO concentration of 10^{-7} (kilograms of CO per kilogram of air). Each of the four schemes were then integrated for five months, with the final concentrations of layer 4 as shown in Figure 12.

Without going into the details of the computations for the winds or the sources and sinks for CO, we simply state that they are realistic for our planet. In fact, with the exception of the upstream scheme, the latitudinal averages of the CO distributions are comparable to observed distributions. The CO problem will be discussed in detail in a separate publication.

As usual the upstream scheme is diffusive, but at least it is very smooth. The second order and fourth order schemes have isolated grid boxes with small concentrations and lines of grid boxes with alternating concentrations. Both of these features are unrealistic; they are not generated by the sources nor the winds, but are caused by the schemes themselves. The pattern for the slopes scheme is very smooth, and at the same time the latitudinal averages are comparable to those of second and fourth order schemes.

CONCLUSION

It is clear from our three dimensional tests that if one is interested in the concentration at a particular location, the slopes scheme is superior to the other schemes. The tracer distributions produced by this scheme are smoother than those of the second order and fourth order schemes, and yet the slopes scheme is not more diffusive than either of those other methods.

We should note that for each step, the slopes scheme requires three times as much computing time as the other schemes. However, much of this computing time can be recouped, because it is possible to take a larger time step with the slopes scheme than with the second or fourth order schemes.

REFERENCES

1. J. D. Mahlman, Preliminary Results from a Three-Dimensional, General Circulation Tracer Model, Proceedings of the Second Conference on the Climatic Impact Assessment Program (A.J. Broderick, Ed.), pp. 321-337, U.S. Department of Transportation, 1972.

2. J. D. Mahlman and R. W. Sinclair, Tests of Various Numerical Algorithms to a Simple Trace Constituent Air Transport Problem, Fate of Pollutants in the Air and Water Environments (I. H. Suffet, Ed.), pp. 223-252, Wiley, New York, 1977.

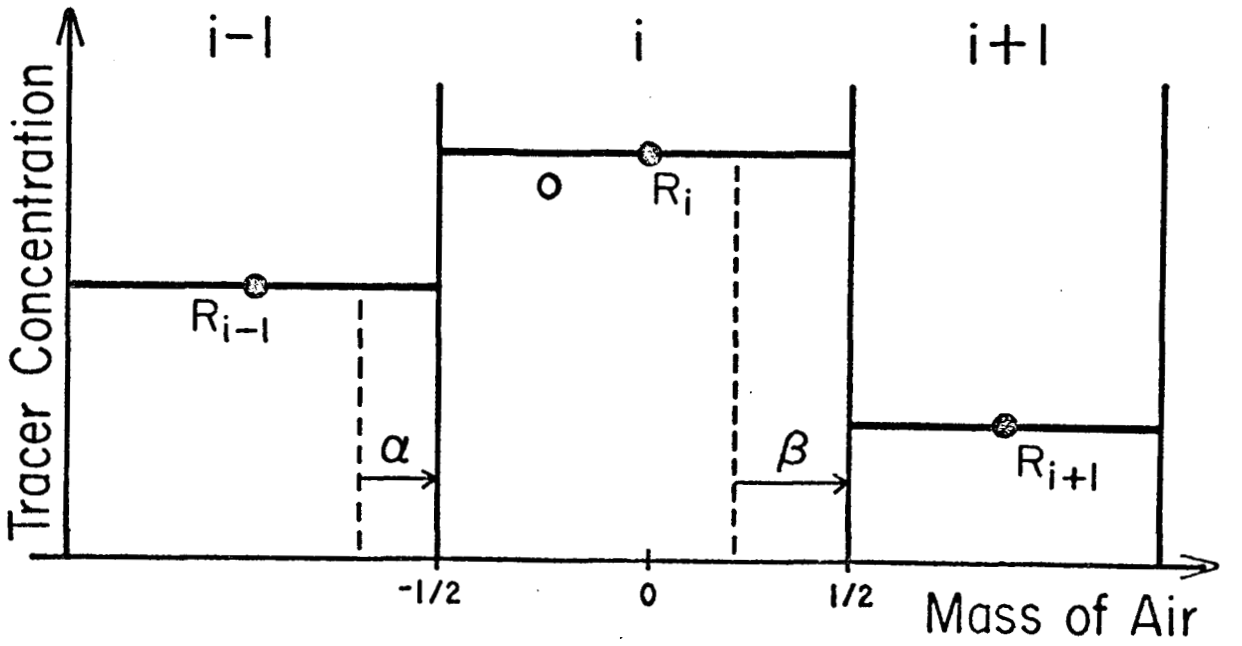

Figure 1. Diagram of the upstream scheme in one dimension. The solid vertical lines are the interfaces of contiguous grid boxes i-1, i and i+1. The abscissa is mass of air normalized by the mass of air in grid box i. The ordinate is tracer concentration. The solid circles are the mean concentrations at the beginning of a time step with values R_{i-1}, R_i and R_{i+1}. The heavy solid lines show the concentration at which tracer is moved. α is the mass of air which moves from grid box i-1 into grid box i during the time step; β is the mass of air which moves from grid box i into grid box i+1. (In this example, both α and β are positive). αR_{i-1} is the mass of tracer which moves from grid box i-1 into grid box i during the time step; βR_i is the mass of tracer which moves from grid box i into grid box i+1. The mean concentration of grid box i at the end of the time step shown by the open circle is $(R_i + \alpha R_{i-1} - \beta R_i)/(1+\alpha-\beta)$.

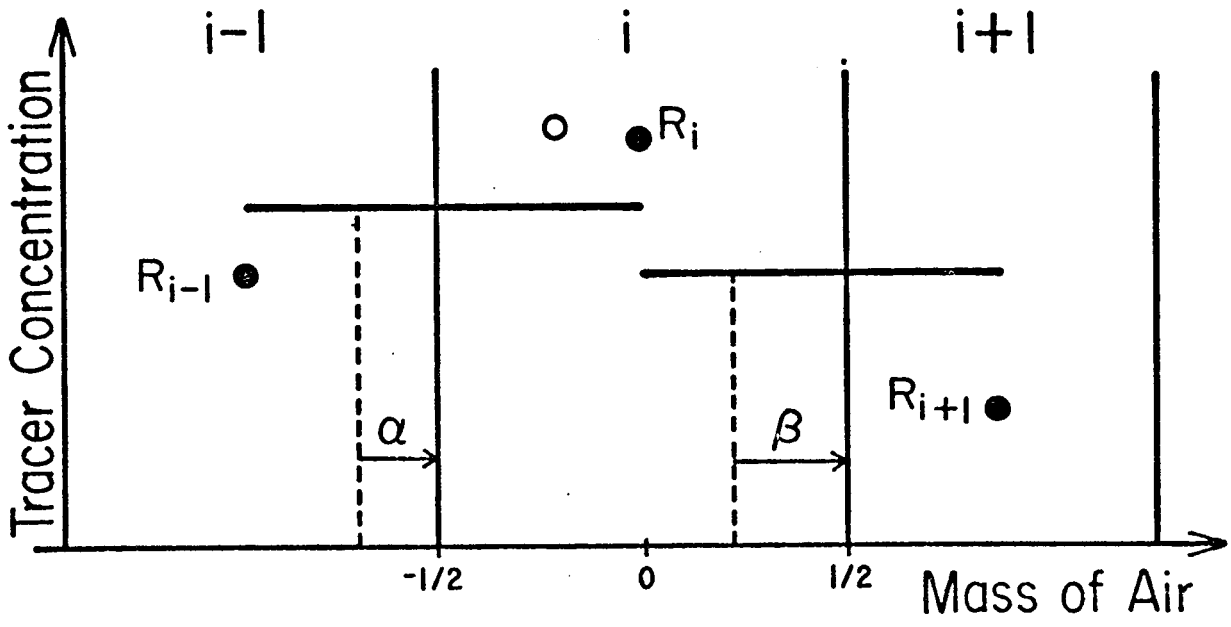

Figure 2. Diagram of the second order scheme in one dimension. For nomenclature refer to Figure 1. $\alpha(R_{i-1}+R_i)/2$ is the mass of tracer which moves from grid box i-1 into grid box i during the time step; $\beta(R_i+R_{i+1})/2$ is the mass of tracer which moves from grid box i into grid box i+1. The mean concentration of grid box i at the end of the time step shown by the open circle is $[R_i+\alpha(R_{i-1}+R_i)/2-\beta(R_i+R_{i+1})/2]/(1+\alpha-\beta)$.

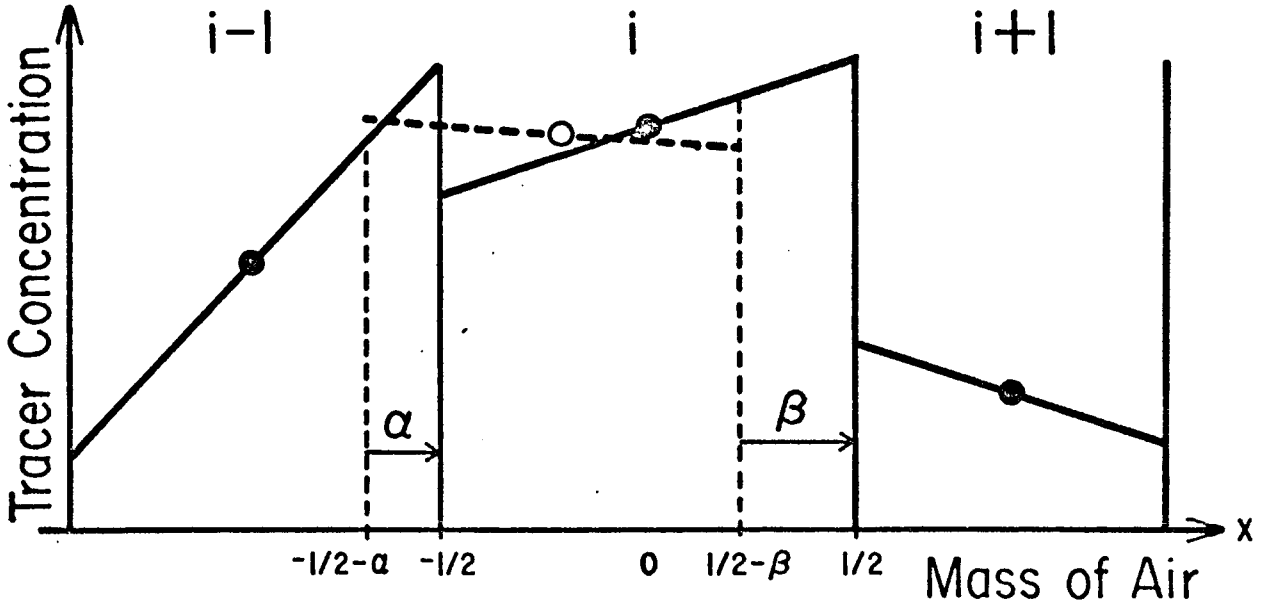

Figure 3. Diagram of the slopes scheme in one dimension. For nomenclature refer to Figure 1. The heavy solid lines indicate the linear distribution of concentration of three grid boxes at the beginning of a time step. They determine a piece-wise linear function f(x). The mass of tracer that moves from grid box i-1 into grid box i during the time step is determined by a trapezoid; the bases are the vertical lines at $-\frac{1}{2}-\alpha$ and $-\frac{1}{2}$, one end is the x-axis, the other end is a heavy solid line. The mass of tracer that moves from i into i+1 is also a trapezoid. The heavy dashed line segment is the least square fit line for the function f(x) in the interval $(-\frac{1}{2}-\alpha, \frac{1}{2}-\beta)$. It determines the linear distribution of grid box i at the end of the time step. By virtue of the least square fit, the center point of the dashed segment coincides with the mean concentration of grid box i at the end of the time step. It is shown by the open circle.

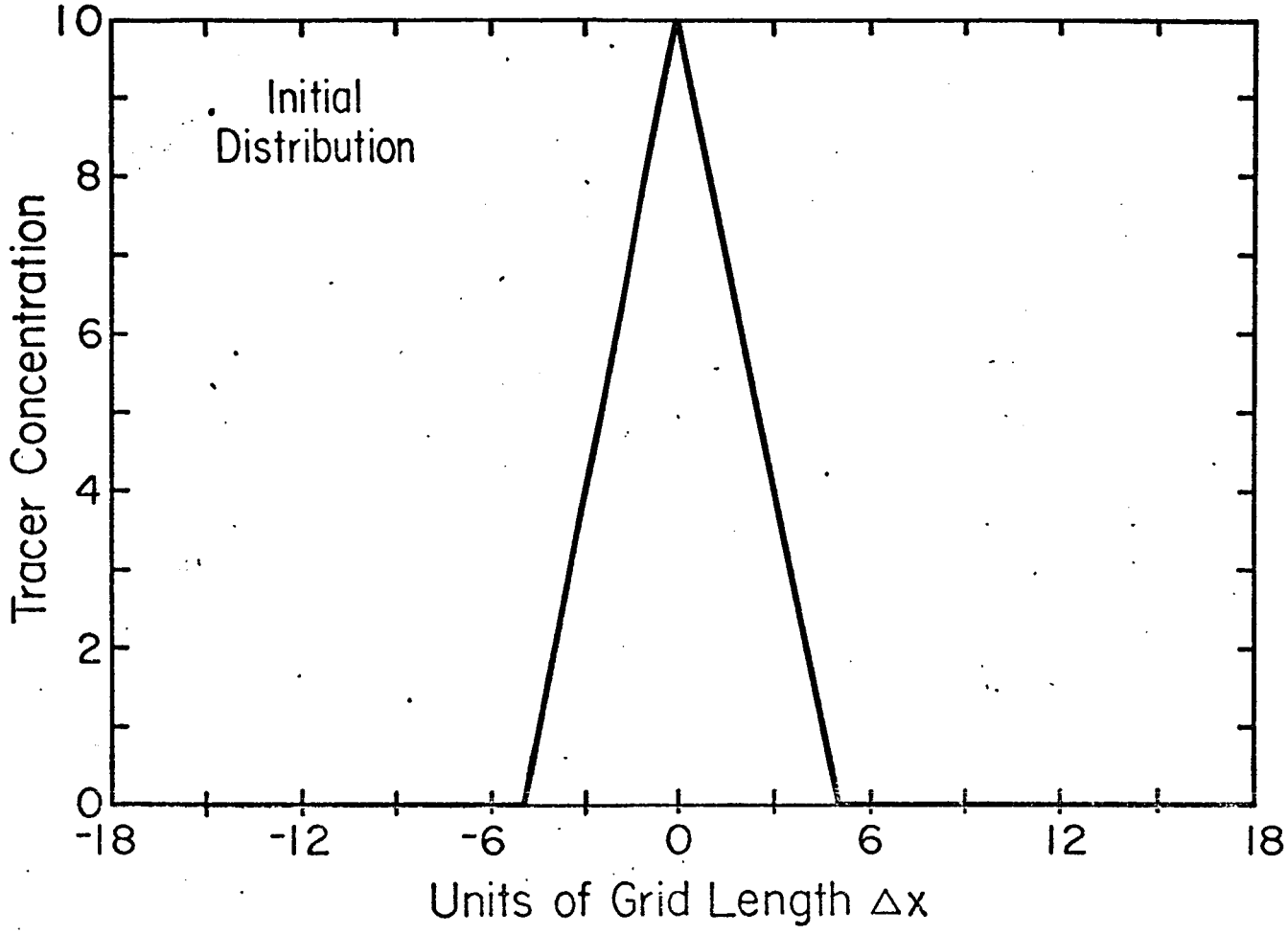

Figure 4. Initial distribution for the one dimensional tests.

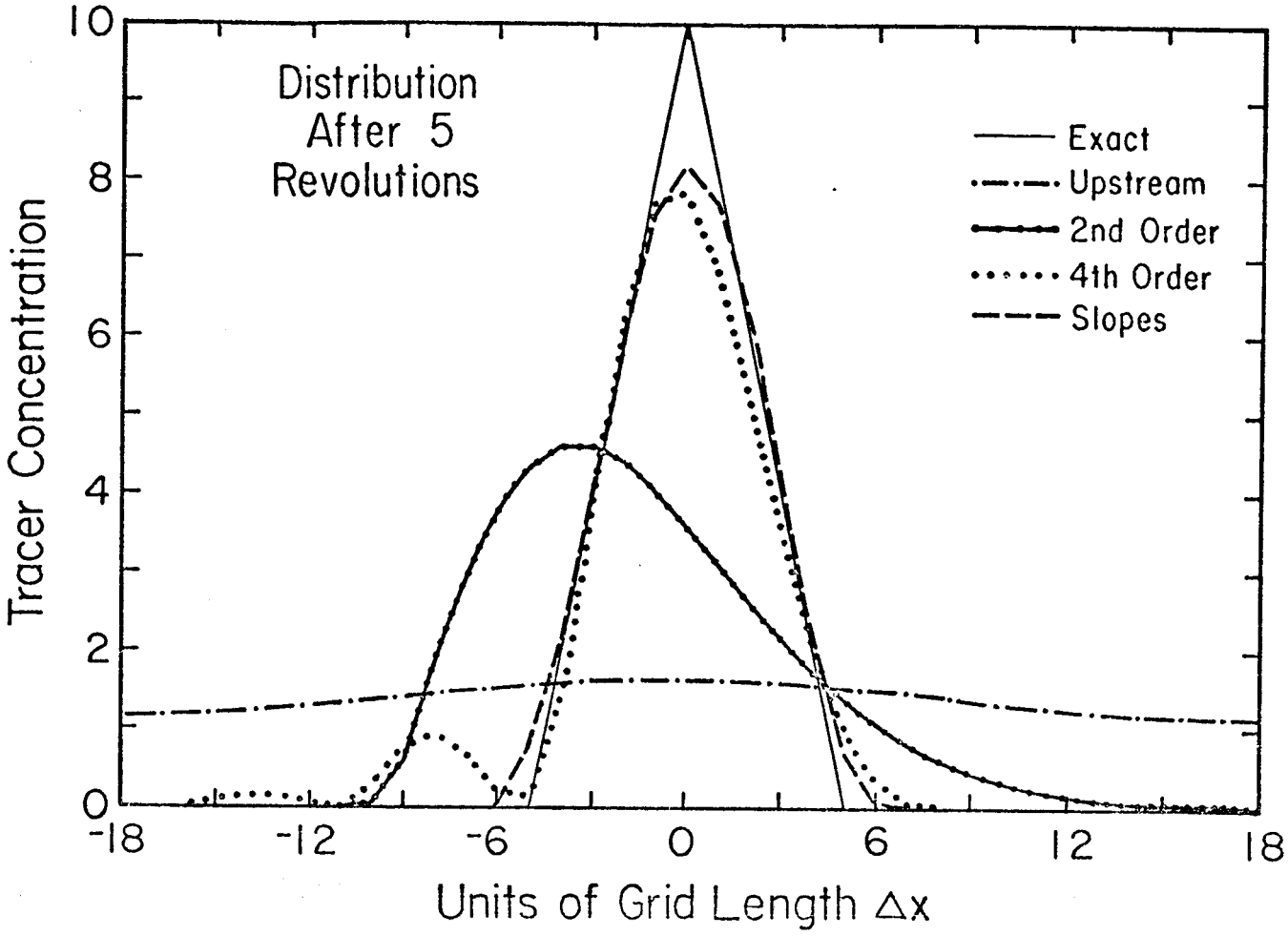

Figure 5. Distribution after 5 revolutions for the one dimensional model. Negative concentrations are prevented by using our stated limits.

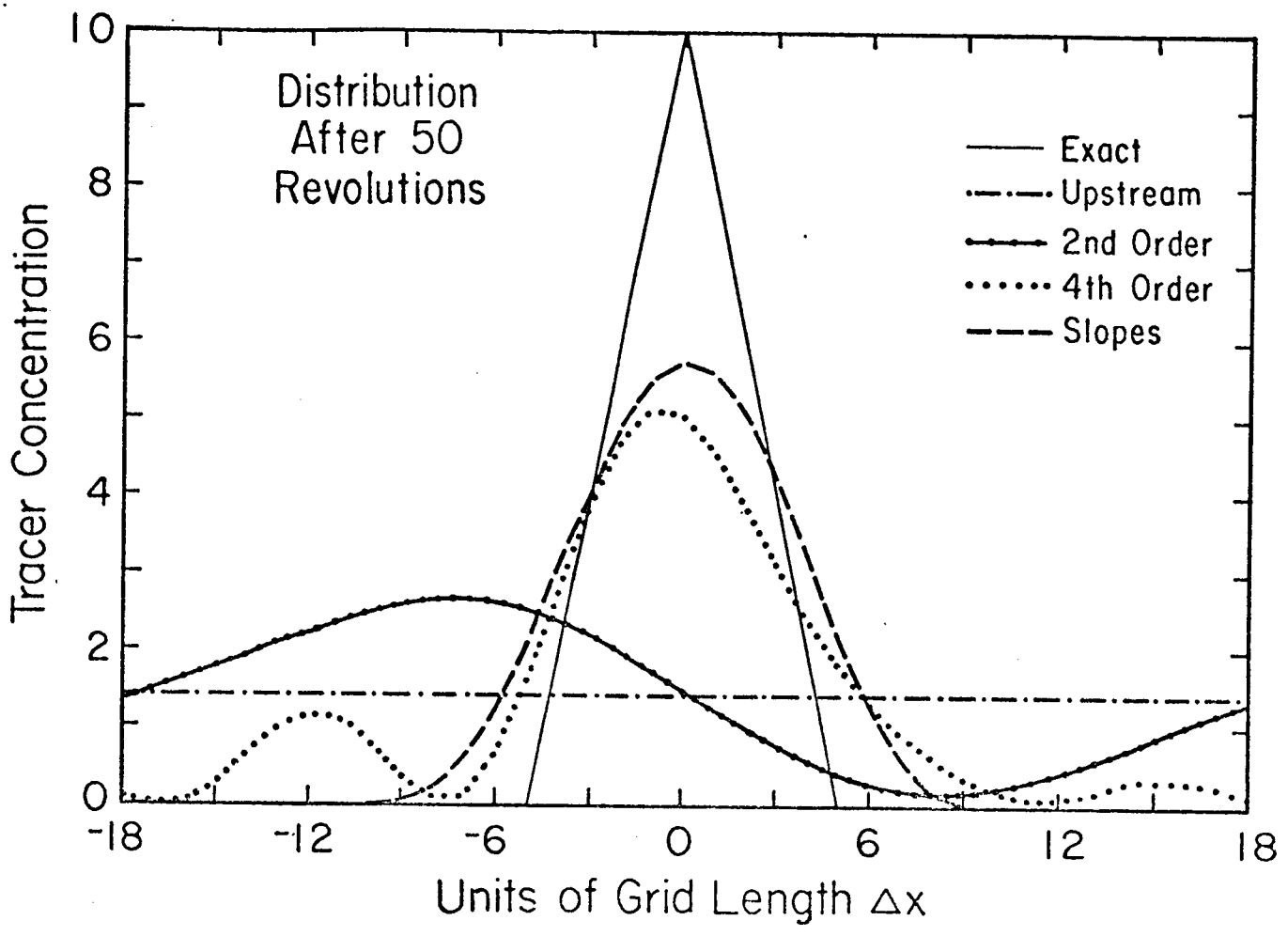

Figure 6. Distribution after 50 revolutions for the one dimensional model. Negative concentrations are prevented by using our stated limits.

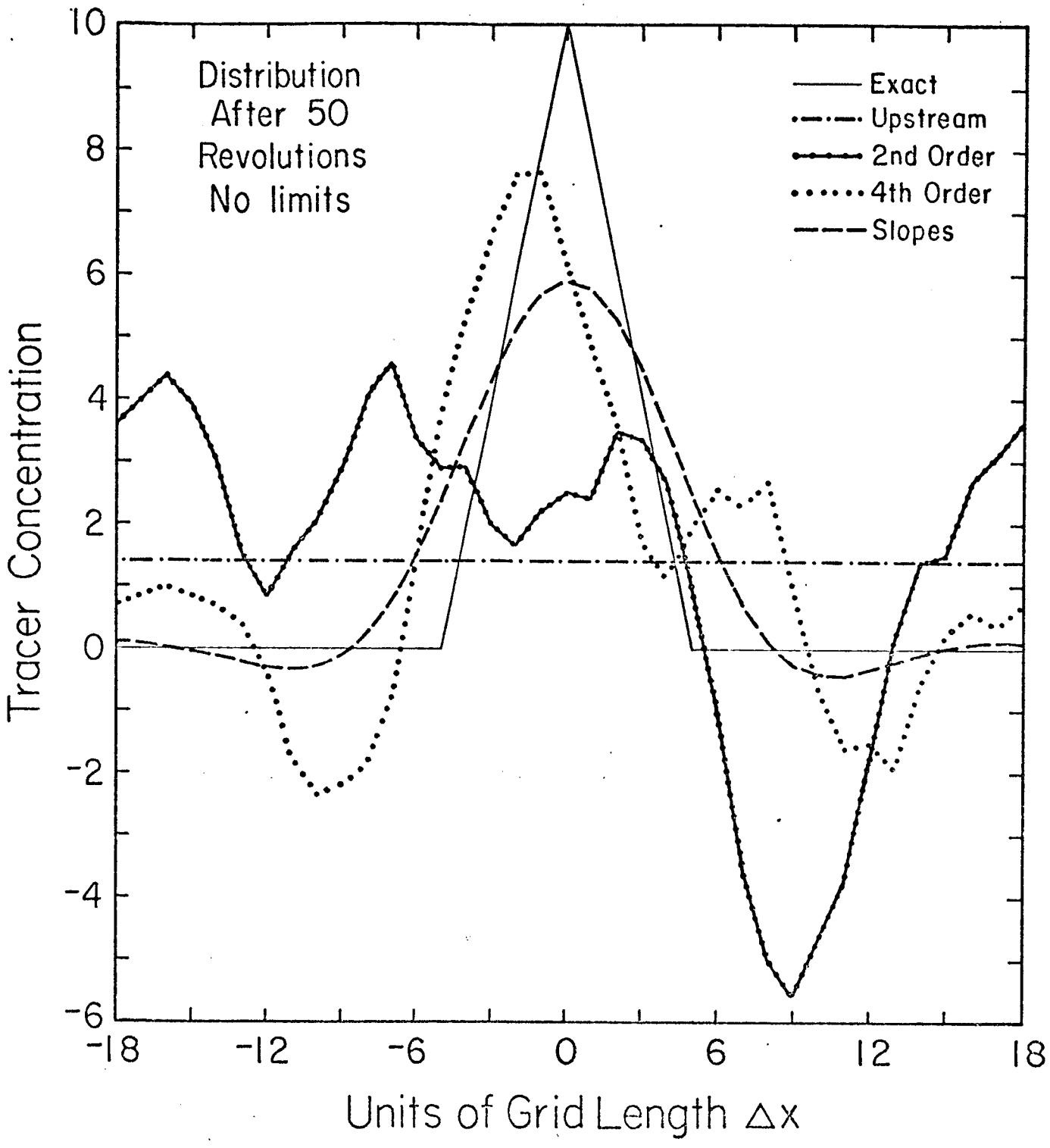

Figure 7. Distribution after 50 revolutions for the one dimensional model. The schemes do not use our limits. Concentrations can be positive or negative.

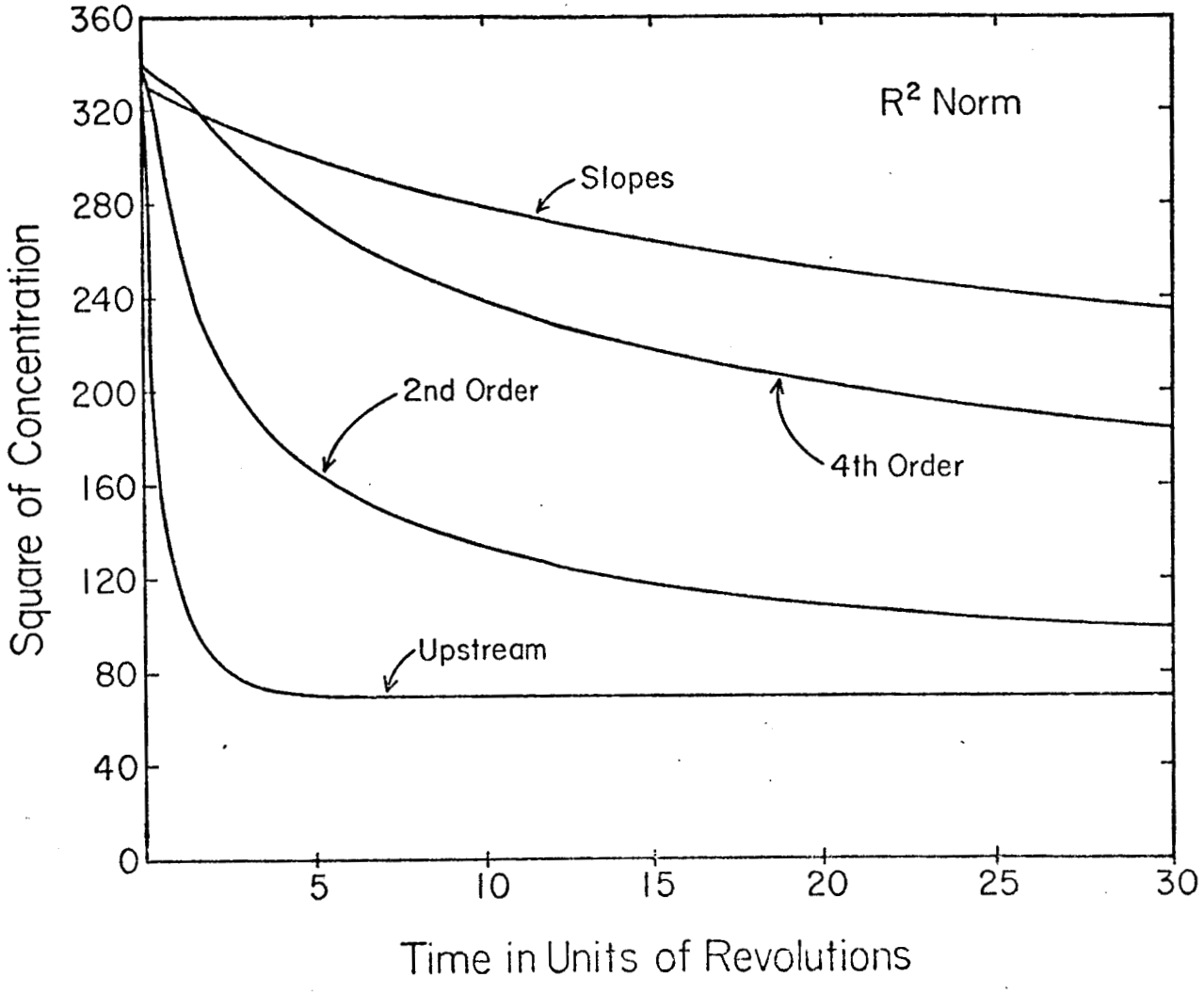

Figure 8. The R^2 norm for the schemes in one dimension as a function of time. The schemes use the stated limits to prevent negative concentrations. The initial state is the wedge (Figure 4) whose R^2 norm is 340.

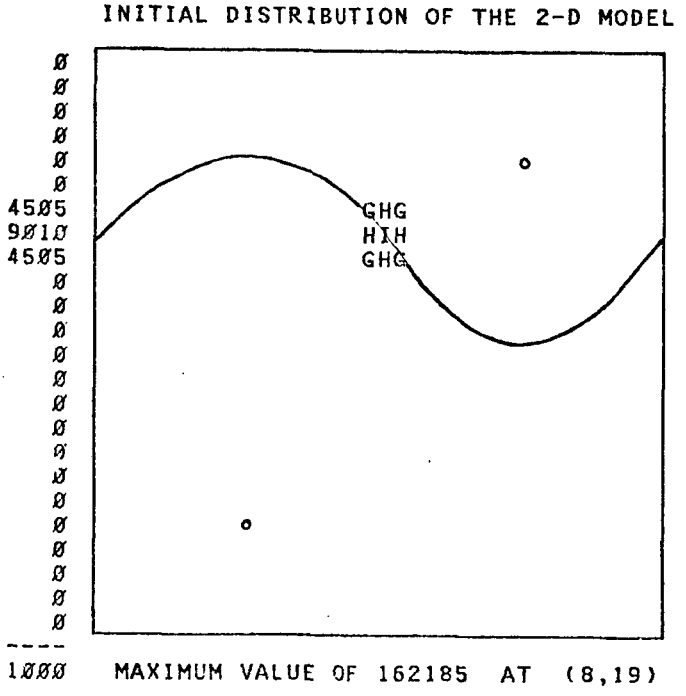

Figure 9. Initial distribution for the two dimensional tests. Latitude and longitude coordinates of the sphere are mapped onto a rectangle; poles of the sphere are mapped onto the top and bottom edges. Numbers on the left indicate the average concentration over a whole latitude. Except for the nine grid boxes, the concentrations are zero. The corner box concentrations of the nine are ¼ the concentration of the center box. The concentrations of the other four are ½ the center concentration. The line shows the path a point would traverse were it to follow our winds exactly. The circles indicate the axis of rotation for the winds.

Figure 10. Distribution after 2 revolutions for the two dimensional model. Negative concentrations are prevented by using our stated limits. Number matrix entries correspond to concentrations from 0 to 32, blanks from 32 to 1024, and letters from 1024 upward. The nine boxes of the initial distribution are outlined.

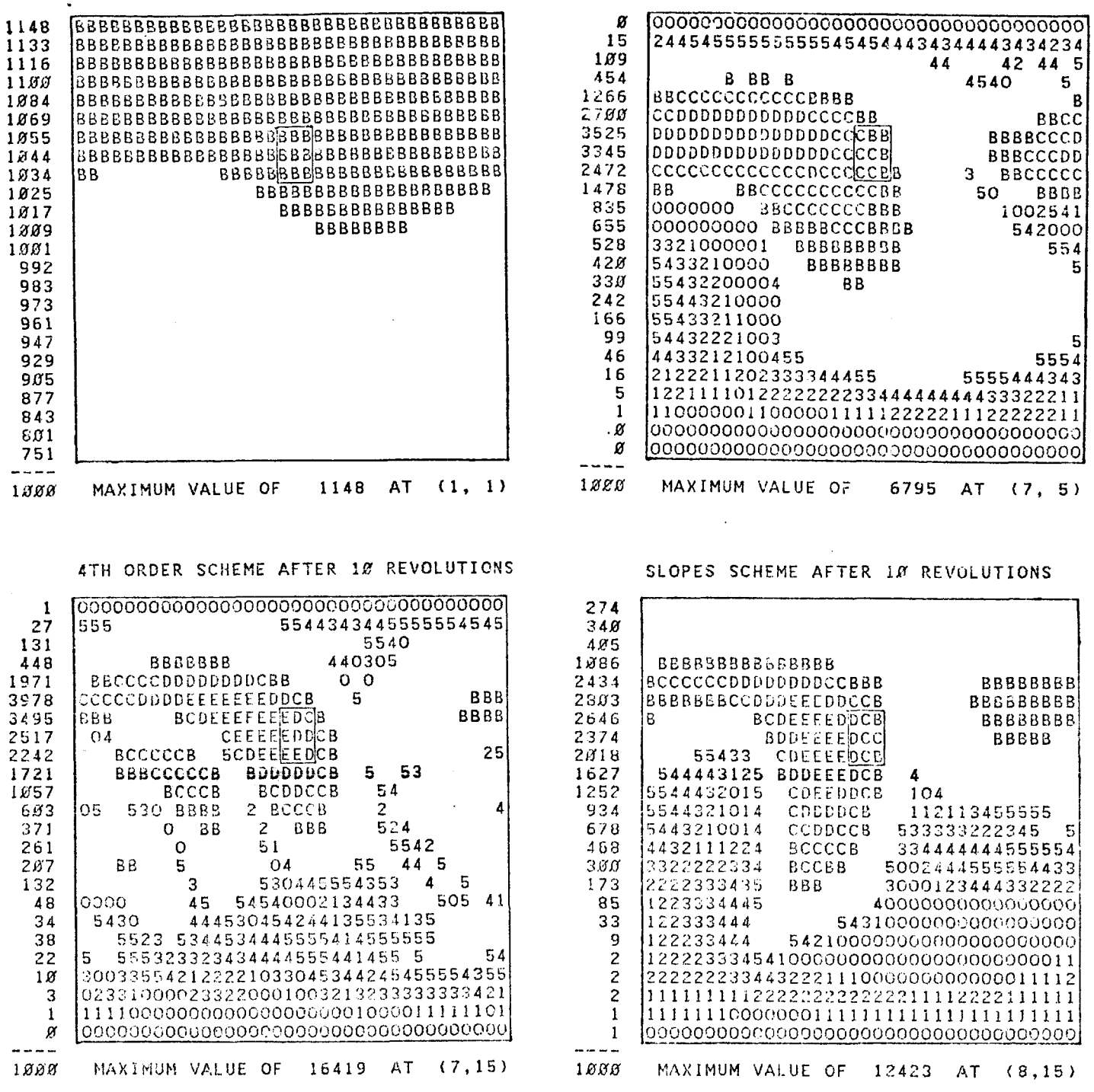

Figure 11. Distribution after 10 revolutions for the two dimensional model. Negative concentrations are prevented by using our stated limits. Number matrix entries correspond to concentrations from 0 to 32, blanks from 32 to 1024, and letters from 1024 upward. The nine boxes of the initial distribution are outlined.

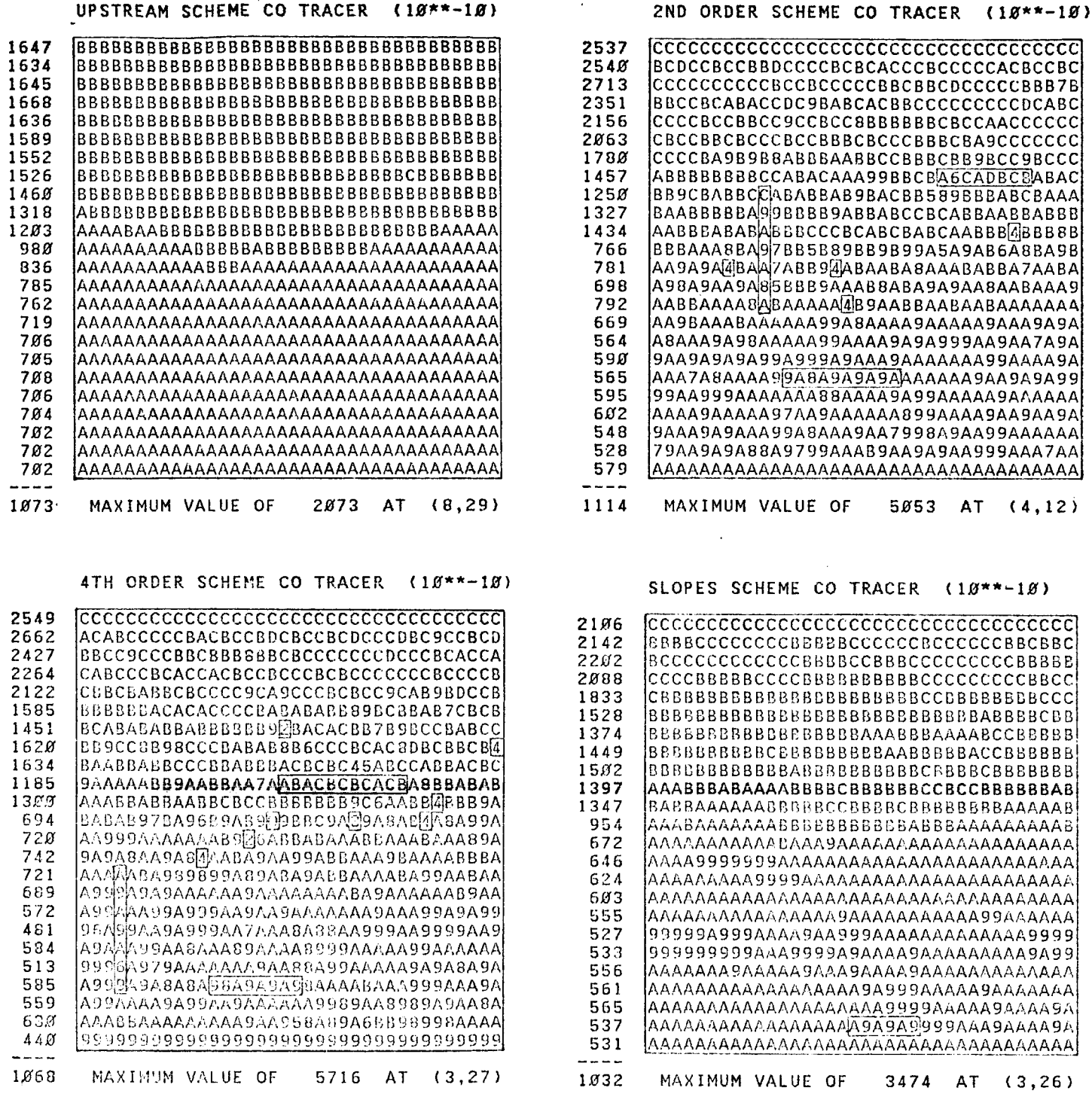

Figure 12. Instantaneous CO distribution of layer 4 of our three dimensional tracer model (in units of 10^{-10} kilograms of CO per kilogram of air). Negative concentrations are prevented by using our stated limits. Grid box entries use our logarithmic base 2 scale. Isolated grid boxes and lines of grid boxes are outlined to show the problems with the schemes.

TABLE I

Frequency of invoking our stated limits

to prevent negative concentrations

	Δt = 1800 seconds			Δt = 3600 seconds		
	E-W	N-S	Vert	E-W	N-S	Vert
Air mass limit, upstream and slopes	0.	0.	0.	.036	0.	0.
Second order limit	1.098	.841	.410	3.532	.946	.413
Fourth order limit	1.298	.986	.626	3.686	1.075	.628
Slopes limit	.035	.123	.274	.034	.117	.244